Many-Body van der Waals Interactions between Graphitic Nanostructures

ARTICLE *in* JOURNAL OF PHYSICAL CHEMISTRY LETTERS · APRIL 2010

Impact Factor: 7.46 · DOI: 10.1021/jz100309m

2 AUTHORS:

Yaroslav Shtogun
University of South Florida
17 PUBLICATIONS **241** CITATIONS
SEE PROFILE

Lilia M. Woods
University of South Florida
104 PUBLICATIONS **1,200** CITATIONS
SEE PROFILE

THE JOURNAL OF PHYSICAL CHEMISTRY Letters

pubs.acs.org/JPCL

Many-Body van der Waals Interactions between Graphitic Nanostructures

Yaroslav V. Shtogun* and Lilia M. Woods*

Department of Physics, University of South Florida, 4202 East Fowler Avenue, Tampa, Florida 33620-5700

ABSTRACT van der Waals interactions between finite-length single-wall carbon nanotubes and graphene nanoribbons are calculated including all many-body contributions. Comparative studies between the total two-, three-, four-, and many-body interaction energies are performed using the coupled dipole model. It is shown that the graphitic dispersive interaction is of truly collective nature. The combined effect of the size of the nanostructures, their anisotropy, orientations, and relative displacements can be captured accurately only when all many-body contributions are taken into account. This is of particular importance for nanotube and nanoribbon axial sliding, where the largest deviations between the few-body and many-body interaction energies are found.

SECTION Nanoparticles and Nanostructures

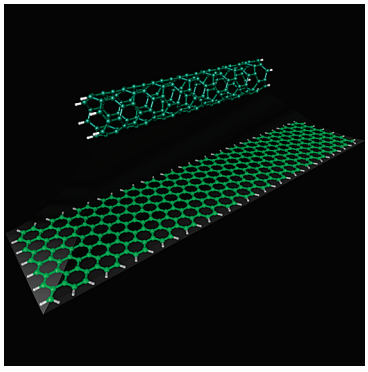

The van der Waals (VDW) dispersion forces are important in many physical, chemical, and biological phenomena. VDW forces are universal since they are present between any atoms, molecules, and/or clusters separated by a distance. They originate from the electromagnetic fluctuations of the electrons in the interacting objects and are of quantum mechanical and dispersive nature. Such forces depend strongly on the geometry, size, atomic nature, and dielectric response of the involved objects.

Currently, VDW interactions have drawn significant interest due to their dominance in many nanostructured, biological, and colloidal materials and devices. For example, the efficient functionality of microelectromechanical systems and nanoelectromechanical systems is directly related to the VDW force.[1,2] Such interactions affect the dispersion of nanoclusters and nanocolloids in suspension.[3] The stability of many nanostructures, more specifically, multiwall carbon nanotubes (CNTs), nanotube ropes and bundles, and graphene nanoribbons (GNRs), is effectively due to these dispersive forces. VDW forces are also responsible for the successful operation of many devices which involve carbon nanotubes. Some examples are carbon nanotube oscillators, actuators, and nanotube-based AFM applications.[4−7] Phenomena such as adsorption and deformation involving carbon nanotubes and nanoribbons can also be a direct consequence of VDW interactions.[7−11]

Thus, understanding the nature of the VDW dispersion forces is of great pertinence for the description and prediction of various phenomena and devices involving graphitic materials. In this regard, taking into account size, geometry, and dielectric response of the involved objects is of particular importance. The VDW interaction is usually calculated within the pairwise summation approximation utilizing the London's formula for the interacting potential $U_{ij} = -C_6/r_{ij}^6$ derived from perturbation theory,[12] where r_{ij} is the distance between atoms i and j and C_6 is a constant. For structures with a relatively small number of atoms, the VDW interaction is calculated by summing over all possible pairs ij, and C_6 is taken from existing experimental data. For larger objects, the summation is substituted with integration over the structure volumes (the Hamaker method[13]). Although these approaches are relatively easy to apply, they ignore many-body, i.e. screening effects assuming $1/r^6$ atomic distance dependence.

To improve the pairwise London approximation, researchers have adapted the Dzyaloshinskii−Lifshitz−Pitaevskii (DLP) method[14] developed for macroscopic objects originally. This approach takes into account screening and retardation (which is significant at large separations where the Casimir force becomes apparent) in a consistent manner, but it has been applied to planar geometries only.[15] As an alternative, the DLP−Derjagun has been developed,[16] which assumes that at very close separations, the objects can be represented as a collection of parallel plates. Then, the resulting VDW interaction is calculated as a sum of the exact DLP result for each macroscopic parallel plate pair. Hence, this is an inherent additive pairwise approach which ignores the discrete atomic structures and assumes the that nanostructures' dielectric response properties are the same as those for bulk.

At the same time, many reports have shown that the microscopic nature of the nanostructures is particularly important for their VDW interactions.[17−19] In the case of graphitic systems, for example, the VDW interaction depends on the mutual orientation of the carbon rings. More specifically, the preferred orientation of graphenes occurs in an AB stacking fashion corresponding to the center of one ring being above a carbon atom from the second one.[20] In addition, the

Received Date: March 9, 2010
Accepted Date: April 6, 2010

DOI: 10.1021/jz100309m | *J. Phys. Chem. Lett.* **2010**, *1*, 1356–1362

polarizability which accounts for the dispersion and absorption properties of each object is significant for the VDW interaction. However, the CNT polarizability, which is determined by their semiconducting or metallic properties through the chirality index, depends strongly on the nanotube length.[21−25]

Most theoretical investigations of CNT interactions have been done for infinitely long structures. These usually involve calculating the VDW interaction using the Hamaker approximation; thus, all many-body effects and discrete atomic nature are ignored.[26,27] Some researchers have also applied the DLP−Derjagun approximation.[28,29] In addition, few results for the VDW interactions between finite-length CNTs using the Hamaker approach have been reported in regards to the carbon nanotube oscillator concept.[30,31] We are not aware of any investigations for GNR VDW interactions.

In this Letter, we focus on the mutual VDW interactions between finite-length carbon nanotubes and graphene nanoribbons in the nonretarded regime. The time delay due the the finite speed of light can be ignored if the size of the objects and their separations are less than 20 nm.[32] The distance between the graphitic nanostructures here will be on the order of several Å, and their size will be less than 70 Å; thus, retardation can be ignored. Our goal is to provide qualitative and quantitative understanding of the collective nature of this phenomenon. We aim at determining the suitability of the two-, three-, and/or four-body approximations for capturing the registry dependence and magnitude of the VDW interaction. For this purpose, we employ the discrete coupled dipole method (CDM),[32,33] which overcomes the difficulties of DLP and DLP−Derjagun approximations for finite nanostructures. This is a unique technique since it takes into account the discrete atomic nature of the structures and it allows the inclusion of all many-body interactions, that is, screening effects are inlcuded.[19,34] In addition, the use of this method is strengthened even more since it gives exactly the same solution originating from quantum mechanical considerations. Within the CDM, the dispersive forces are formulated as a result of the collective interaction between all atoms of the system. The advantages of this approach are that all many-body effects, the types of different atoms, and their specific locations are taken into account simultaneously. In addition, the method allows the total energy to be represented as a sum of various many-body terms; thus, one can determine the importance of each contribution separately.

Within the CDM, each finite CNT or GNR structure is modeled as an arrangement of N dipoles positioned at the location of each atom. The corresponding energy is calculated from the zero-point ground-state fluctuations of all atomic dipoles comprising the objects. The polarizability of every atom for a particular structure is described by the isotropic Drude model as $\alpha_i(\omega) = \alpha_{0i}\omega_{0i}^2/(\omega_{0i}^2 - \omega^2)$, where α_{0i} is the static polarizability and ω_{0i} is the characteristic frequency of the ith atom ($i = 1/N$). There is a dipole moment $\mathbf{p}_i$ at each atomic site i generated from the induced electric field $\mathbf{E}_i^{\mathrm{ind}}$ from the rest of the atoms if no external electric field is applied. Therefore, using $\mathbf{p}_i = \alpha_i\mathbf{E}_i^{\mathrm{ind}}$, where $\mathbf{E}_i^{\mathrm{ind}} = \sum_{j=1, j\neq i}\mathbf{T}_{ij}\mathbf{p}_j$, $\mathbf{T}_{ij} = (3\mathbf{r}_{ij}\mathbf{r}_{ij} - r_{ij}^2\mathbf{I})/r_{ij}^5$ ($\mathbf{T}_{ij} = 0$ if $i = j$) is the dipole−dipole interaction tensor, with $\mathbf{r}_{ij}$ as the radius vector between those atoms and $\mathbf{I}$ as the 3×3 identity matrix, one obtains the following set of $3N$ coupled equations

$$\begin{bmatrix} \mathbf{I}/\alpha_{01} & -\mathbf{T}_{12} & \cdots & -\mathbf{T}_{1N} \\ -\mathbf{T}_{21} & \mathbf{I}/\alpha_{02} & \cdots & -\mathbf{T}_{2N} \\ \vdots & \vdots & \ddots & \vdots \\ -\mathbf{T}_{N1} & \cdots & \cdots & \mathbf{I}/\alpha_{0N} \end{bmatrix} \begin{bmatrix} \mathbf{p}_1 \\ \mathbf{p}_2 \\ \vdots \\ \mathbf{p}_N \end{bmatrix}$$
$$= \omega^2 \begin{bmatrix} \mathbf{I}/(\alpha_{01}\omega_{01}^2) & \mathbf{0} & \cdots & \mathbf{0} \\ \mathbf{0} & \mathbf{I}/(\alpha_{02}\omega_{02}^2) & \cdots & \mathbf{0} \\ \vdots & \vdots & \ddots & \vdots \\ \mathbf{0} & \mathbf{0} & \cdots & \mathbf{I}/(\alpha_{0N}\omega_{0N}^2) \end{bmatrix} \begin{bmatrix} \mathbf{p}_1 \\ \mathbf{p}_2 \\ \vdots \\ \mathbf{p}_N \end{bmatrix} \quad (1)$$

This self-consistent system corresponds to the general eigenvalue problem, which we solve using standard algorithms. We are particularly interested in the positive eigenvalues ω_n, which give the allowed coupled modes of the entire structure. The many-body VDW energy of the system is determined as $U = \hbar\sum_{n=1}^{3N}(\omega_n - \omega_{0i})/2$. Then, the total many-body VDW energy between two nanostructures A and B with atoms N_A and N_B, respectively, is found using

$$U_{TN} = \hbar\sum_{n=1}^{3N_A+3N_B}\omega_n/2 - \hbar\sum_{n=1}^{3N_A}\omega_n/2 - \hbar\sum_{n=1}^{3N_B}\omega_n/2 \quad (2)$$

where the appropriate self-energies are subtracted. U_{TN} represents the total VDW interaction energy between the two systems, which accounts for all many-body effects, the atomic corrugation, and geometry of each structure.

The structures of interest here are finite single-wall CNTs and graphitic GNRs. A single-wall carbon nanotube is obtained by rolling a graphene sheet into a cylinder with a diameter ~nm. A typical CNT usually has a length of several μm, and it is characterized by a chirality index (n,m).[35] A GNR is obtained by cutting a stripe from a graphene sheet[36] or by unzipping a CNT along its axis.[37] GNRs are also quasi-one-dimensional structures with chirality-dependent transport behavior, but they are planar. Considering the fact that there are many ways to cut the graphene sheet, in the present work, we focus on GNRs obtained by unfolding a specific CNT along its axis. Thus, GNRs are characterized with the same chiral indices as those used for the CNTs from which they are obtained.[38,39]

We present calculations of VDW interactions using eq 2 for the following graphitic structures derived from a (6,0) CNT with passivated free bonds by H atoms. The length along the z-axis for the longer structures is 68.92 Å corresponding to 16 translational unit cells along z-axis (CNT_{16}, GNR_{16}) and for the shorter ones is 30.58 Å corresponding to 7 translational unit cells along z-axis (CNT_7, GNR_7). For all studied configurations, the initial surface-to-surface separation between the two surfaces is taken to be $D_0 = 3.4$ Å (Figure 1), which is the approximate equilibrium distance between graphene sheets in graphite and between carbon nanotubes in nanotube bundles.[40,41] The highly symmetric carbon ring mutual orientations are denoted in Figure 1d as top (T), bridge (B), and hollow (H). The T and H are the well-known AB- and AA-stacking in graphite, respectively,[20] while the B was shown to be preferred for some benzene-derived molecules adsorbed

DOI: 10.1021/jz100309m | J. Phys. Chem. Lett. 2010, 1, 1356–1362

THE JOURNAL OF PHYSICAL CHEMISTRY Letters
pubs.acs.org/JPCL

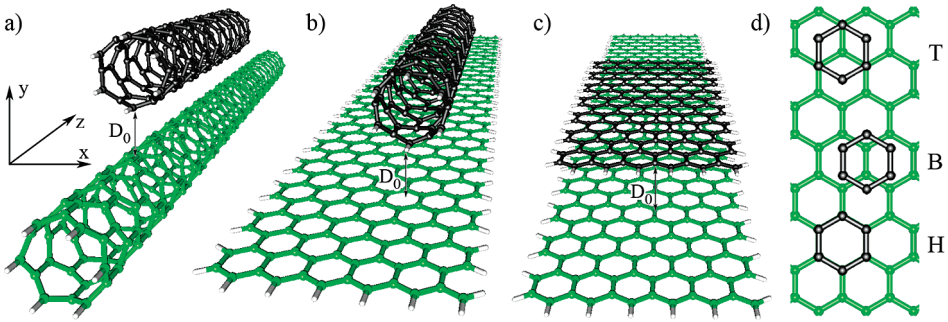

Figure 1. (a) Two (6,0) nanotubes (CNT_{16}−CNT_7); (b) (6,0) nanoribbon and (6,0) nanotube (GNR_{16}−CNT_7); (c) two (6,0) nanoribbons (GNR_{16}−GNR_7); (d) stacking symmetry of the hexagonal rings; T-top, B-bridge, and H-hollow. The surface-to-surface distance is D_0 = 3.4 Å.

on graphitic systems.[42] It turns out that the T, H, and B stackings are also important for the strength of the VDW interaction in terms of the particular nanostructures and the type of mutual displacement.

To facilitate the calculations, a set of parameters for the static polarizabilities and characteristic frequencies must be taken. Many studies evaluating VDW interactions usually rely on the atomic values for α_{0i} and ω_{0i}.[18,26,43] This means that the atomic characteristics stay the same as they form a molecule or a cluster, and the molecular static polarizability is obtained by simply summing the atomic polarizabilities. However, it has been repeatedly shown that this concept is not correct, and in many instances, choosing atomic α_{0i} and ω_{0i} does not describe relevant experimental data.[44−46] In our calculations, we take the following parameters for the CNT static polarizabilities and characteristic frequencies: α_H = 0.19 Å^3, α_C = 1.25 Å^3, $\omega_H = 1.41 \times 10^{16}$ rad/s, and $\omega_C = 1.85 \times 10^{16}$ rad/s. These parameters have been shown to be successful when describing properties of cylindrically circular CNTs.[22] For GNRs, we take static polarizabilities and characteristic frequencies appropriate for planar aromatic molecules,[45,46] α_H = 0.25 Å^3, α_C = 0.85 Å^3, $\omega_H = 1.41 \times 10^{16}$ rad/s, and $\omega_C = 1.85 \times 10^{16}$ rad/s.

Figure 2 presents results for the calculated total many-body VDW interaction energy U_{TN} for short and long CNTs, a short CNTand a long GNR, and short and long GNRs as a function of surface-to-surface distance D_0 when the two structures have a common axial direction and are moved away from each other. For such a situation, the relative orientation of the hexagonal rings (H stacking for two CNTs and CNT/GNR and B stacking for two GNRs) stays the same for all values of D_0. One sees that the interaction energy decreases monotonically as the distance is increased and $|U_{TN}(CNT_{16}-CNT_7)| < |U_{TN}(GNR_{16}-CNT_7)| < |U_{TN}(GNR_{16}-GNR_7)|$ for all D_0. The fact that the attraction between the two GNRs is the strongest is due to the larger aspect ratio since the overlap between the nanoribbons is the largest. Consequently, due to the CNT cylindrical curvature, fewer atoms are found at a closer distance, and $U_{TN}(CNT_{16}-CNT_7)$ is the weakest.

Besides the separation of graphitic structures by moving them away from one another, other possible configurations can be considered. Here, we study the sliding of one nanostructure along the *x*- and *z*-axis with respect to the other (Figure 3). The interaction energy for the displacement along the axial

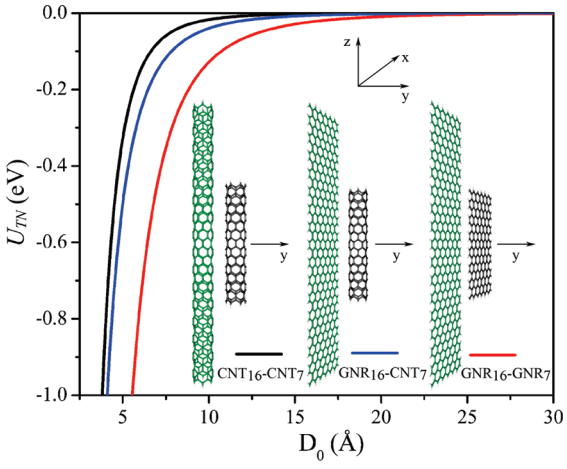

Figure 2. Total many-body VDW energy as a function of surface-to-surface separation distance D_0 for two nanotubes (CNT_{16}−CNT_7), nanoribbon and nanotube (GNR_{16}−CNT_7), and two nanoribbons (GNR_{16}−GNR_7). The studied configurations and the direction of displacement are also shown.

direction is of particular importance for modeling of carbon nanotube and graphitic nanoribbon bearing devices, which have been proposed and/or demonstrated recently.[6,30,31] In addition, U_{TN} for the relative displacement for all directions can be used to understand the corrugation of graphitic surfaces with different curvatures or even find mechanisms to distinguish nanotubes or nanoribbons by helical angles via interaction with larger graphitic surfaces.[47−49]

Figure 3 shows that there are oscillatory-like features for the axial sliding. These are much more pronounced for the CNT/CNT and GNR/GNR relative motions. For example, the difference between the minimum and maximum energies for GNRs is $|U_{TN}^{min} - U_{TN}^{max}|$ = 334 meV, while $|U_{TN}^{min} - U_{TN}^{max}|$ = 3 meV for the CNT/GNR system. These features are attributed to a purely geometrical effect arising from the preferential orientation of the carbon rings. It is interesting to note that the strongest interaction corresponding to U_{TN}^{min} occurs when the carbon rings are in H stacking (Figure 1d), while the U_{TN}^{max} is associated with the B stacking for the CNT/GNR and GNR/GNR *z*-sliding. For the CNT/CNT, the oscillations in U_{TN} are rather irregular with altering T and H preferred stackings. This is unlike the case of the graphene/graphene VDW interaction,

DOI: 10.1021/jz100309m | *J. Phys. Chem. Lett.* 2010, *1*, 1356–1362

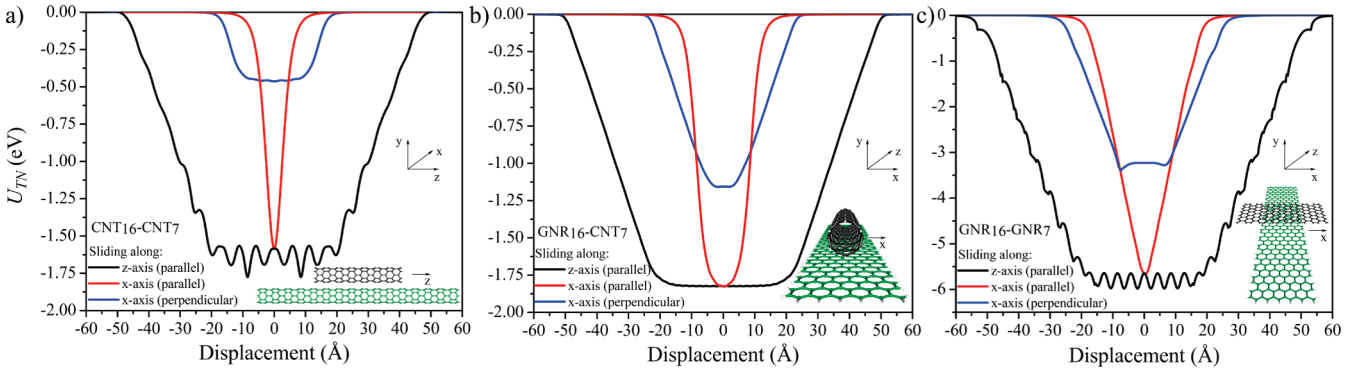

Figure 3. Total many-body VDW energy as a function of displacement for (a) two nanotubes ($CNT_{16}-CNT_7$), (b) nanoribbon and nanotube ($GNR_{16}-CNT_7$), and (c) two nanoribbons ($GNR_{16}-GNR_7$) in three sliding geometries. The displacement corresponds to the relative separation between the centers of mass of the nanostructures along the relevant axis. "Parallel" refers to a common axial direction for the two nanostructures, and "perpendicular" refers to the case when the nanostructure axes are perpendicular. The sliding geometries are depicted in the insets. The surface-to-surface distance along the *y*-axis is kept constant at −3.4 Å.

which is strongest for T stacking of the hexagonal rings (AB stacking). The oscillatory-like features are still present for larger displacements ($> |20|$ Å), but they are much less pronounced as the overlap area between the structures decreases. This behavior is lost for graphitic structure slidings along the *x*-axis, for which U_{TN} decreases monotonically for larger displacement.

Comparing the strengths of the VDW interaction betweens the different structures shows that the strongest attraction occurs between two GNRs regardless of their orientation. In fact, U_{TN} for GNRs with a parallel *z*-axis is ∼3.4 times stronger than U_{TN} when there is at least one CNT involved. Thus, the planar geometry is a key to much more stable configurations due to the greater surface overlap. This indicates that it is much more difficult to separate two GNRs than two CNTs or a CNT from a GNR.

We further investigate the question of the important contributions originating from the inherently collective nature of this phenomenon. Many of the reported studies dealing with the CNT and graphene do not take many-body interactions into account but rather use the continuous Hamaker approach.[2,26,27,30,31] While this may be appropriate for materials which are weakly polarizable with isotropic polarizability and relatively small screening effects, it is not clear if such a two-body VDW interaction is applicable to graphitic nanostructures. It is well-known that graphitic nanostructures do not possess these features; they have chirality- and length-dependent anisotropic polarizabilities and screening effects.[21−25] At the same time, their VDW interaction is registry-dependent, which is not realistically described by the pairwise model.[47−49] In fact, comparing the interaction potential obtained from ab initio calculations and the one from the London approach shows that the two-body potential is much too smooth to capture the corrugation effects for intertube displacements.[48] This happens because the two-body potential is isotropic since it depends on the atomic distances only. Thus, in general, this approximation is not suitable to describe the anisotropic CNT and GNR response properties.

The standard approach to improve the interaction in finite structures has been to simply add the three-body VDW force using the Axilrod−Teller−Muto expression.[50,51] Usually, this is sufficient for noble gases for which the three-body terms become prominent at small distances.[52] For nanoclusters made out of other materials, such as Na, Au, Ag, or Si, studies indicate that the inclusion of terms beyond the two-body and three-body contributions is necessary to describe the VDW interaction correctly.[3,19,52−54]

The CDM approach allows one to take into account simultaneously all relevant factors, such as discrete atomic positions and collective excitations for finite systems, in a natural way. Furthermore, we can calculate the contribution from different *n*-body terms and determine how each one affects the VDW energy *U* using the binomial theorem and constructing a power expansion in terms of the atomic polarizabilities $U = \sum_{n=2}^{N} U_n$.[55,56] Each U_n contains $N(N-1)...(N+1-n)/n!$ terms. Thus, the number of terms for each successive *n*-body interaction is ∼*N* times larger than the previous one. At the same time, $U_n \approx 1/r^{3n}$. For large separations, the contribution for three-body, four-body, and higher-order interactions diminishes greatly due to that distance dependence. However, for close separations, like the equilibrium distances in graphitic nanostructures, the $\sim N^n$ dependence of each U_n can overcome the $1/r^{3n}$ functionality and give substantial contributions to the total VDW energy.[52] This competing behavior between the large number of terms for U_n interactions and the relatively small distances between graphitic materials is a key factor in the inherently many-body nature of their VDW forces.

To give a quantitative description of this issue, we evaluate the total two-body (U_{T2}), three-body (U_{T3}), four-body (U_{T4}), and many-body U_{TN} using eq 2 for two (6,0) CNTs, (6,0) CNT and (6,0) GNR, and two (6,0) GNRs with five unit cells along the *z*-axis (22.06 Å) when the nanostructures are moved apart along the *y*-direction. The results are given in Figure 4. It is evident that for two CNTs (Figure 4a), the two-body interaction overestimates the many-body U_{TN}. Adding U_{T3} decreases U_{T2}, while adding U_{T4} increases $U_{T2} + U_{T3}$ as compared to U_{TN}. For the CNT and GNR interaction (Figure 4b), it seems that U_{T2} is almost the same as U_{TN}, and the effects of U_{T3} and U_{T4} have similar trends as those for the two CNTs. For the GNRs, however, the two-body interaction is smaller than the many-body U_{TN}, and its deviation is larger than the U_{T2}/U_{TN}

DOI: 10.1021/jz100309m | J. Phys. Chem. Lett. 2010, 1, 1356–1362

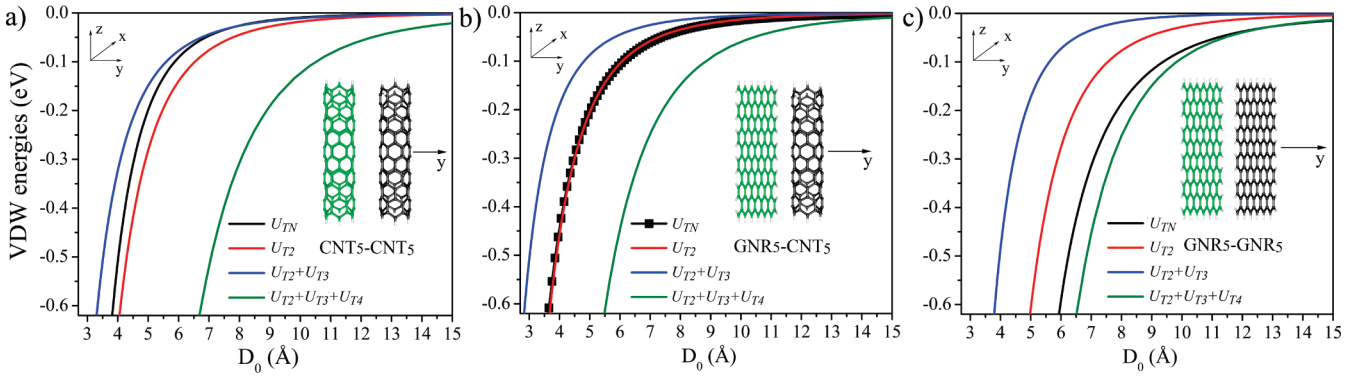

Figure 4. VDW energies corresponding to U_{TN}, U_{T2}, $U_{T2} + U_{T3}$, and $U_{T2} + U_{T3} + U_{T4}$ interactions as a function of separation distance D_0 for (a) two (6,0) nanotubes (CNT_5-CNT_5), (b) (6,0) nanoribbon and (6,0) nanotube (GNR_5-CNT_5), (c) and two (6,0) nanoribbons (GNR_5-GNR_5) with five translational unit cells.The relative geometries are also shown as insets.

deviation for the two CNTs. Our calculations show that for all considered systems, U_{T3} is always positive; thus, when added to the negative U_{T2}, $U_{T2} + U_{T3}$ decreases. U_{T4} is always negative, and due to the large number of terms, it becomes significant at distances of $D_0 < 20$ Å. When the separation between the nanostructures becomes comparable or larger than their size, the largest contribution to U_{TN} is mainly from the two-body interaction.

These results suggest that, since $U_n \approx N^n$ for larger nanostructures at their equilibrium distances (~3.4 Å), the contribution from each n-body interaction is bigger than the previous U_{n-1} term. At the same time, the altering signs of the different U_n (negative for n odd and positive for n even) from the binomial expansion can cause severe cancellations in $U = \Sigma_n U_n$. This balance between the magnitude of each independent term and its sign is strongly dependent on the size of the particular nanostructures and their mutual displacements.

Further investigations show the importance of the many-body nature of the VDW long-ranged interactions for the different sliding displacements. In Figure 5, we show our results for the two-body and three-body terms when the shorter nanostructure slides along the longer one keeping a common axial direction. The deviations of U_{T2} from U_{TN} are rather different for the considered cases. When there is a CNT involved (Figure 5a, b), U_{T2} always overestimates U_{TN}. Also, for two CNTs, the registry dependence of the two-body VDW energy is much less pronounced than the one of the total energy. There are also nonlinearities in U_{TN} which are missing in U_{T2}; the largest difference between H and T stackings in U_{TN} is 0.21 eV, while it is only 0.01 eV in U_{T2}. This oscillatory-like behavior is at a much smaller scale for both U_{T2} and U_{TN} when the CNT slides along a GNR. For two GNRs sliding along the axial direction, however, U_{T2} underestimates U_{TN} by ~20% at a displacement of less than |20| Å (Figure 5c). The U_{T2} oscillatory features are also much less pronounced when the two structures overlap (compare $|U_{T2}^{min} - U_{T2}^{max}| = 0.02$ eV and $|U_{TN}^{min} - U_{TN}^{max}| = 0.33$ eV), and they are lost when the GNRs do not overlap completely at a displacement of more than |20| Å. In all cases, adding U_{T3} and/or U_{T4} does not provide any remedy to the two-body interaction; on the contrary, it results in even bigger discrepancies.

These findings are of particular importance to practical situations involving graphitic nanostructure axial sliding, such as CNT oscillators and rotating actuators, which operate at equilibrium surface-to-surface distances. Practically all descriptions for nanotube oscillators, for example, have been obtained using models based on the two-body VDW approximation with constants appropriate for graphite.[30] Our results, however, indicate that such an approach does not describe

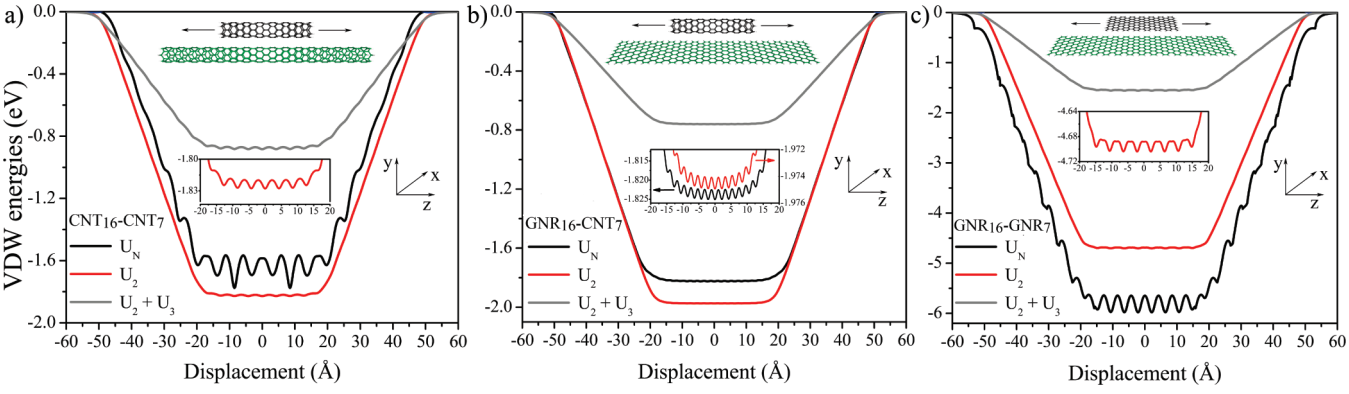

Figure 5. VDW energies for U_{TN}, U_{T2}, and $U_{T2} + U_{T3}$ energies as a function of the center of mass displacement along the z-direction for (a) two nanotubes (CNT_{16}−CNT_7), (b) nanoribbon and nanotube (GNR_{16}−CNT_7), and (c) two nanoribbons (GNR_{16}−GNR_7).The insets show the sliding geometries with the surface-to-surface separation distance of $D_0 = 3.4$ Å.

the magnitude of the interaction nor the strength of the corrugation correctly. In addition, corrugation effects are directly related to the friction in the sliding CNT systems, which have been estimated to be small compared to the mutual VDW force.[5] We suggest that modeling CNT oscillations and rotations has to be revised taking into account the full many-mody force for more realistic modeling of the sliding motion and friction losses in the system.

In summary, we have calculated VDW interactions between graphitic nanostructures, demonstrating the manifestation of the relation between the inherently collective nature of this phenomenon together with the anisotropy, geometry, and mutual orientation of these materials. The total VDW energy is several times stronger for planar systems because of the larger aspect ratio as compared to the VDW energy of cylindrically circular nanotubes with similar size. The description of the interactions between finite-size CNTs and GNRs by the London approach at distances comparable to the size of the structures is not sufficient. Due to its isotropic atomic distance dependence, the two-body interaction is much too smooth to capture the relative alignment effects of the graphitic surfaces. This is most pronounced for axial sliding for which there is a greater surface overlap. Simply adding the first few contributions coming from the three- and four-body terms does not provide any improvements; rather, they give even larger deviations from the total energy in terms of overscreening or underscreening depending on the considered particular structures and orientations. Thus, long-ranged interactions between graphitic nanostructures are of truly collective nature. Therefore, all many-body interactions are necessary in order to capture the correct magnitude and corrugation of the VDW interactions between graphitic nanostructures.

AUTHOR INFORMATION

Corresponding Author:

*To whom correspondence should be addressed. E-mail: lwoods@cas.usf.edu (L.M.W.); yshtogun@cas.usf.edu (Y.V.S.).

ACKNOWLEDGMENT We acknowledge financial support from the Department of Energy under Contract DE-FG02-06ER46297.

REFERENCES

(1) Delrio, F. W.; Deboer, M. P.; Knapp, J. A.; Reedy, E. D.; Clews, P. J.; Dunn, M. L. The Role of van der Waals Forces in Adhesion of Micromachined Surfaces. *Nat. Mater.* **2005,** *4*, 629–634.

(2) Dequesnes, M.; Rotkin, S. V.; Aluru, N. R. Calculation of Pull-In Voltage for Carbon-Nanotube-Based Nanoelectromechnical Switches. *Nanotechnology* **2002,** *13*, 120–122.

(3) Gatica, M. S.; Cole, M. W.; Velegol, D. Designing Van der Waals Forces Between Nanocolloids. *Nano Lett.* **2005,** *5*, 169–173.

(4) Sazonova, V.; Yaish, Y.; Ustunel, H.; Roundy, D.; Arias, T. A.; McEuen, P. L. A Tunable Carbon Nanotube Electromechanical Oscillator. *Nature* **2004,** *431*, 284–287.

(5) Kang, J. W.; Song, K. O.; Hwang, H. J.; Jiang, Q. Nanotube Oscillator Based on a Short Single-Walled Carbon Nanotube Bundle. *Nanotechnology* **2006,** *17*, 2250–2258.

(6) Bourlon, B.; Glattli, D. C.; Miko, C.; Forro, L.; Bachtold, A. Carbon Nanotube Based Bearing for Rotational Motions. *Nano Lett.* **2004,** *4*, 709–712.

(7) Wilson, N. R.; Macpherson, J. V. Carbon Nanotube Tips for Atomic Force Microscopy. *Nat. Nanotechnol.* **2009,** *4*, 483–491.

(8) Ruoff, R. S.; Tersoff, J.; Lorents, D. C.; Subramoney, S.; Chan, B. Radial Deformation of Carbon Nanotubes by van der Waals Forces. *Nature* **1993,** *364*, 514–516.

(9) Wang, Q.; Johnson, J. K. Optimization of Carbon Nanotube Arrays for Hydrogen Adsorption. *J. Phys. Chem. B* **1999,** *103*, 4809–4813.

(10) Hertel, T.; Walkup, R. E.; Avouris, P. Deformation of Carbon Nanotubes by Surface van der Waals Forces. *Phys. Rev. B* **1998,** *58*, 13870–13873.

(11) Law, M.; Sirbully, D. J.; Johnson, J. C.; Goldberger, J.; Saykally, R. J.; Yang, P. Nanoribbon Waveguides for Subwavelength Photonics Integration. *Science* **2004,** *305*, 1269–1273.

(12) London, F. Zur Theorie und Systematik der Molekularkrafte. *Z. Phys.* **1930,** *63*, 245–279.

(13) Hamaker, H. C. The London—van Der Waals Attraction Between Spherical Particles. *Physica* **1937,** *4*, 1058–1072.

(14) Dzyaloshinskii, I. E.; Lifshitz, E. M.; Pitaevskii, L. P. The General Theory of van der Waals Forces. *Adv. Phys.* **1961,** *10*, 165–209.

(15) Bordag, M.; Klimchitskaya, G. L.; Mohideen, U.; Mostepanenko, V. M. *Advances in the Casimir Effect*; Oxford University Press: Oxford, U.K., 2009.

(16) Derjaguin, B. Analysis of Friction and Adhesion IV. The Theory of the Adhesion of Small Particles. *Kolloid-Z.* **1934,** *69*, 155–164.

(17) Girard, G.; Labeke, D. V.; Vigoureux, J. M. van der Waals Forces Between a Spherical Tip and a Solid Surface. *Phys. Rev. B* **1989,** *40*, 12133–12139.

(18) Gravil, P. A.; Devel, M.; Lambin, Ph.; Bouju, X.; Girard; Lucas, A. A. Adsorption of C_{60} Molecules. *Phys. Rev. B* **1996,** *53*, 1622–1629.

(19) Kim, H. Y.; Sofo, J. O.; Velegol, D.; Cole, M. W.; Lucas, A. A. van der Waals Forces Between Nanoclusters: Importance of Many-Body Effects. *J. Chem. Phys.* **2006,** *124*, 074504/1–074504/4.

(20) Charlier, J. C.; Michenaud, J. P.; Gonze, X. First-Principles Study of the Electronic Properties of Simple Hexagonal Graphite. *Phys. Rev. B* **1992,** *46*, 4531–4533.

(21) Langlet, R.; Devel, M.; Lambin, Ph. Computation of the Static Polarizabilities of Multi-Wall Carbon Nanotubes and Fullerites Using a Gaussian Regularized Point Dipole Interaction Model. *Carbon* **2006,** *44*, 2883–2895.

(22) Jensen, L.; Astrand, P.; Mikkelsen, K. V. The Static Polarizability and Second Hyperpolarizability of Fullerenes and Carbon Nanotubes. *J. Phys. Chem. A* **2004,** *108*, 8795–8800.

(23) Jensen, L.; Schmidt, O. H.; Mikkelsen, K. V.; Astrand, P. Static and Frequency-Dependent Polarizability Tensors for Carbon Nanotubes. *J. Phys. Chem. B* **2000,** *104*, 10462–10466.

(24) Slepyan, G. Ya.; Maksimenko, S. A.; Yevtushenko, O.; Gusakov, A. V. Electrodynamics of Carbon Nanotubes: Dynamic Conductivity, Impedance Boundary Conditions, and Surface Wave Propagation. *Phys. Rev. B* **1999,** *60*, 17136–17149.

(25) Gumbs, G.; Aizin, G. R. Collective Excitations in a Linear Periodic Array of Cylindrical Nanotubes. *Phys. Rev. B* **2002,** *65*, 195407/1–195407/6.

(26) Girifalco, L. A.; Hodak, M.; Lee, R. S. Carbon Nanotubes, Buckyballs, Ropes, and a Universal Graphitic Potential. *Phys. Rev. B* **2000,** *62*, 13104–13110.

DOI: 10.1021/jz100309m | *J. Phys. Chem. Lett.* **2010,** *1*, 1356–1362

(27) Parsegian, V. A. *van der Waals Forces: A Handbook for Biologist, Chemists, Engineers, and Physicist*; Cambridge University Press: Cambridge, U.K., 2005.
(28) Bordag, M.; Geyer, B.; Klimchitskaya, G. L.; Mostepanenko, V. M. Lifshitz-Type Formulas for Graphene and Single-Wall Carbon Nanotubes: van der Waals and Casimir Interactions. *Phys. Rev. B* **2006,** *74*, 205431/1–205431/9.
(29) Rajter, R. F.; Podgornik, R.; Parsegian, V. A.; French, R. H.; Ching, W. Y. van der Waals—London Dispersion Interactions for Optically Cylinders: Metallic and Semiconducting Single-Wall Carbon Nanotubes. *Phys. Rev. B* **2007,** *76*, 045417/1–045417/16.
(30) Zheng, Q.; Liu, J.; Jiang, Q. Excess van der Waals Interaction Energy of a Multiwalled Carbon Nanotube with an Extruded Core and the Induced Core Oscillation. *Phys. Rev. B* **2002,** *65*, 245409/1–245409/6.
(31) Hilder, T. A.; Hill, J. M. Oscillating Carbon Nanotori along Carbon Nanotubes. *Phys. Rev. B* **2007,** *75*, 125415/1–125415/8.
(32) Cole, M. W.; Velegol, D.; Kim, H. Y.; Lucas, A. A. Nanoscale van der Waals interactions. *Mol. Simul.* **2009,** *35*, 849–866.
(33) Purcell, E. M.; Pennypacker, C. R. Scattering and Absorption of Light by Nonspherical Dielectric Grains. *Astrophys. J.* **1973,** *186*, 705–714.
(34) Kim, H. Y.; Kent, P. R. C. van der Waals Forces: Accurate Calculation and Assessment of Approximate Methods in Dielectric Nanocolloids up to 16 nm. *J. Chem. Phys. Lett.* **2009,** *131*, 144705/1–144705/5.
(35) Satio, R.; Dresselhause, G.; Dresselhause, M. *Physical Properties of Carbon Nanotubes*; Imperial Collage Press: London, 2003.
(36) Jia, X.; Hofman, M.; Meunier, V.; Sumpter, B. G.; Campos-Delgado, J.; Romo-Herrera, J. M.; Son, H.; Hsieh, Y. P.; Reina, A.; Kong, J.; et al. Controlled Formation of Sharp Zigzag and Armchair Edges in Graphitic Nanoribbons. *Science* **2009,** *323*, 1701–1705.
(37) Kosynkiv, D. V.; Higginbotham, A. L.; Sinitskii, A.; Lomeda, J. R.; Dimiev, A. Longitudinal Unzipping of Carbon Nanotubes to Form Graphene Nanoribbons. *Nature* **2009,** *458*, 872–876.
(38) Barone, V.; Hod, O.; Scuseria, G. E. Electronic Structure and Stability of Semiconducting Graphene Nanoribbons. *Nano Lett.* **2006,** *6*, 2748–2754.
(39) Obradovic, B.; Kotlyar, R.; Heinz, F.; Matagne, P.; Rakshit, P.; Giles, M. D.; Stettler, M. A. Analysis of Graphene Nanoribbons as a Channel Material for Field-Effect Transistors. *Appl. Phys. Lett.* **2006,** *88*, 142102/1–142102/3.
(40) Iijima, S. Helical Microtubules of Graphitic Carbon. *Nature* **1991,** *354*, 56–58.
(41) Ge, M.; Sattler, K. Bundles of Carbon Nanotubes Generated by Vapor-Phase Growth. *Appl. Phys. Lett.* **1994,** *64*, 710–711.
(42) Woods, L.; Badescu, S.; Reinecke, T. Adsorption of Simple Benzene Derivatives on Carbon Nanotubes. *Phys. Rev. B* **2007,** *75*, 155415/1–155415/9.
(43) Kim, H. Y.; Sofo, J. O.; Velegol, D.; Cole, M. W.; Lucas, A. A. van der Waals Dispersion Forces Between Dielectric Nanoclusters. *Langmir* **2007,** *23*, 1735–1740.
(44) Silberstein, L. Molecular Refractivity and Atomic Interaction. *Philos. Mag.* **1917,** *33*, 92–128.
(45) Applequist, J.; Carl, J. R.; Fung, K. An Atom Dipole Interaction Model for Molecular Polarizability. Application to Polyatomic Molecules and Determination of Atomic Polarizability. *J. Am. Chem. Soc.* **1972,** *94*, 2952–2960.
(46) Jensen, L.; Astrand, P. O.; Osted, A.; Kongsted, J.; Mikkelsen, K. V. Polarizability of Molecular Clusters as Calculated by a Dipole Interaction Model. *J. Chem. Phys.* **2002,** *116*, 4001–4010.
(47) Buldum, A.; Lu, J. P. Atomic Scale Sliding and Rolling of Carbon Nanotubes. *Phys. Rev. Lett.* **1999,** *83*, 5050–5053.
(48) Kolmogorov, A. N.; Crespi, V. H. Registry-Dependent Interlayer Potential for Graphitic Systems. *Phys. Rev. B* **2005,** *71*, 235415/1–235415/6.
(49) Kolmogorov, A. N.; Crespi, V. H. Nanotube—Substrate Interactions: Distingvishing Carbon Nanotubes by the Helical Angle. *Phys. Rev. Lett.* **2004,** *92*, 085503/1–085503/4.
(50) Axilrod, B. M.; Teller, E. Interaction of the van der Waals Type Between Three Atoms. *J. Chem. Phys.* **1943,** *11*, 299–300.
(51) Muto, Y. Forces Between Non-Polar Molecules. *J. Phys. Math. Soc. Jpn.* **1943,** *17*, 629–631.
(52) Hermann, A.; Krawczyk, R. P.; Lein, M.; Schwerdtfeger, P. Convorgence of the Many-Body Expansion of Interaction Potentials: From van der Waals to Covalent and Metallic Systems. *Phys. Rev. A* **2007,** *76*, 013202/1–013202/10.
(53) Kaplan, I. G.; Santamaria, R.; Novaro, O. Non-Additive Forces in Atomic Clusters. The Case of Ag_n. *Mol. Phys.* **1995,** *84*, 105–114.
(54) Bravo-Perez, G.; Garzon, I. L.; Novaro, O. Ab Initio Study of Small Gold Clusters. *J. Mol. Struct.: THEOCHEM* **1999,** *493*, 255–231.
(55) Bade, W. L. Drude-Model Calculation of Dispersion Forces. I. General Theory. *J. Chem. Phys.* **1957,** *27*, 1280–1284.
(56) MacRury, T. B.; Linder, B. Many-Body Aspects of Physical Adsorption. *J. Chem. Phys.* **1971,** *54*, 2056–2066.

DOI: 10.1021/jz100309m | *J. Phys. Chem. Lett.* **2010,** *1*, 1356–1362